IBS Center
for Climate Physics

계절 내 극한기후 발생 전망과 이를 지배하는 주요인자들

(APEC기후센터 2021 기후예측워크숍)

Kyung-Ja Ha[1,2,3]

[1] Center for Climate Physics, Institute for Basic Science, Busan, 46241, South Korea
[2] Department of Climate System, Pusan National University, Busan, 46241, South Korea
[3] Department of Atmospheric Sciences, Pusan National University, Busan, 46241, South Korea

Was the abnormal rainfall in Korea linked to Global Warming?

61 stations: individual

Total rainfall in extreme events averaged over 61 stations

Number of days per year (99th percentile) in extreme events averaged over 61 stations

Maximum rainfall value among 61 stations

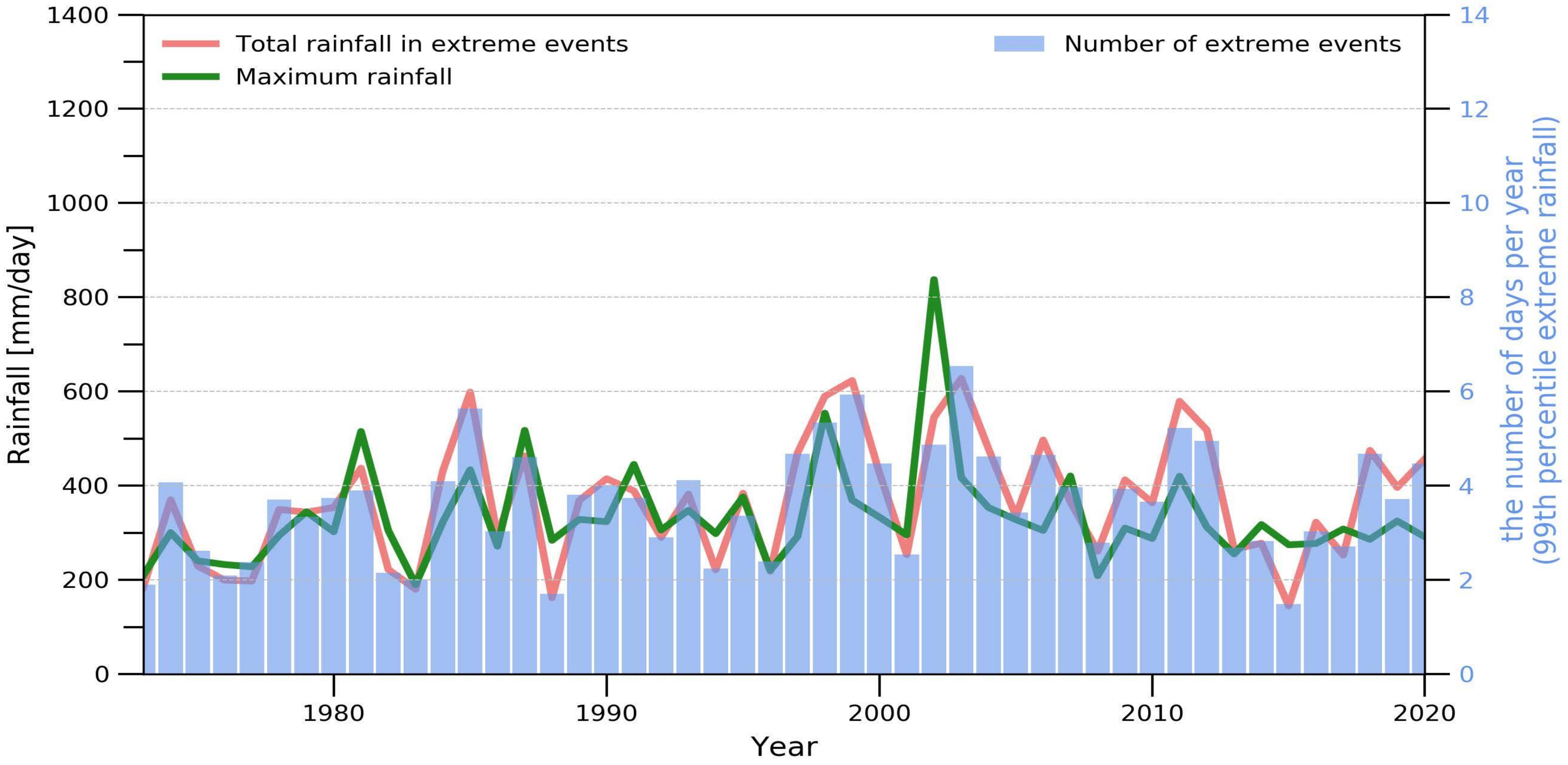

Linear trend, Time of emergence

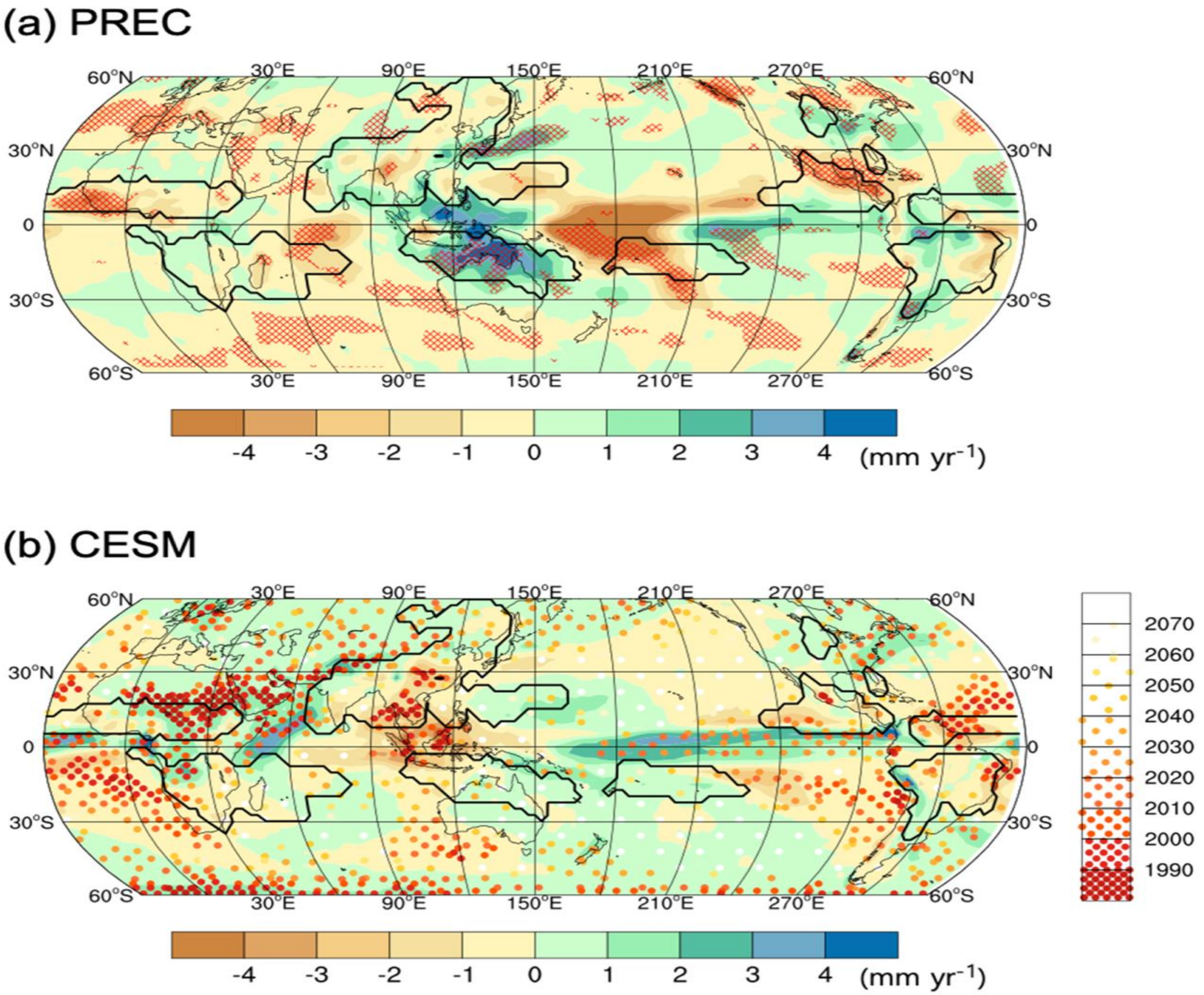

Ha et al., 2020 (ERL)

Moisture budget for physical process

$$(P-E) \cong -\frac{1}{g\rho_w}\int_{100hPa}^{1000hPa} \nabla\cdot(\bar{V}\bar{q})dp - \frac{1}{g\rho_w}\int_{100hPa}^{1000hPa} \nabla\cdot(\overline{V'q'})dp \qquad (1)$$

Moisture flux convergence by mean flow

Moisture flux convergence by transient eddies

→ *Overbars indicate the mean values and primes departure from its mean values.*

,where $\bar{V}$ is the horizontal wind vector and q is specific humidity.

$$(P-E) \cong -<\nabla\cdot(\bar{V}\bar{q})> - <\nabla\cdot(\overline{V'q'})> \qquad (2)$$

; $\langle\cdot\rangle$ indicates a mass-weighted vertical integral.

$$\delta(P-E) \cong -<\nabla\cdot(\delta\bar{V}\bar{q}_{clim})> - <\nabla\cdot(\bar{V}_{clim}\delta\bar{q})> - <\nabla\cdot(\delta\bar{V}\delta\bar{q})> - <\nabla\cdot\delta(\overline{V'q'})> \qquad (3)$$

; δ represents monthly anomalies from the monthly climatological mean.

Dynamic [DY] **Thermodynamic [TH]**

$$\delta(P-E) \cong \underbrace{-<\delta\bar{V}\cdot\nabla\bar{q}_{clim}>}_{①} \underbrace{-<\bar{q}_{clim}\nabla\cdot\delta\bar{V}>}_{②} \underbrace{-<\bar{V}_{clim}\cdot\nabla\delta\bar{q}>}_{③} \underbrace{-<\delta\bar{q}\nabla\cdot\bar{V}_{clim}>}_{④}$$

$$\underbrace{-<\delta\bar{V}\cdot\nabla\delta\bar{q}>}_{⑤} \underbrace{-<\delta\bar{q}\nabla\cdot\delta\bar{V}>}_{⑥} \underbrace{-<\nabla\cdot\delta(\overline{V'q'})>}_{⑦}$$

Quadratic [QD]

Disentangling impacts of dynamic and thermodynamic components on late summer rainfall anomalies in East Asia

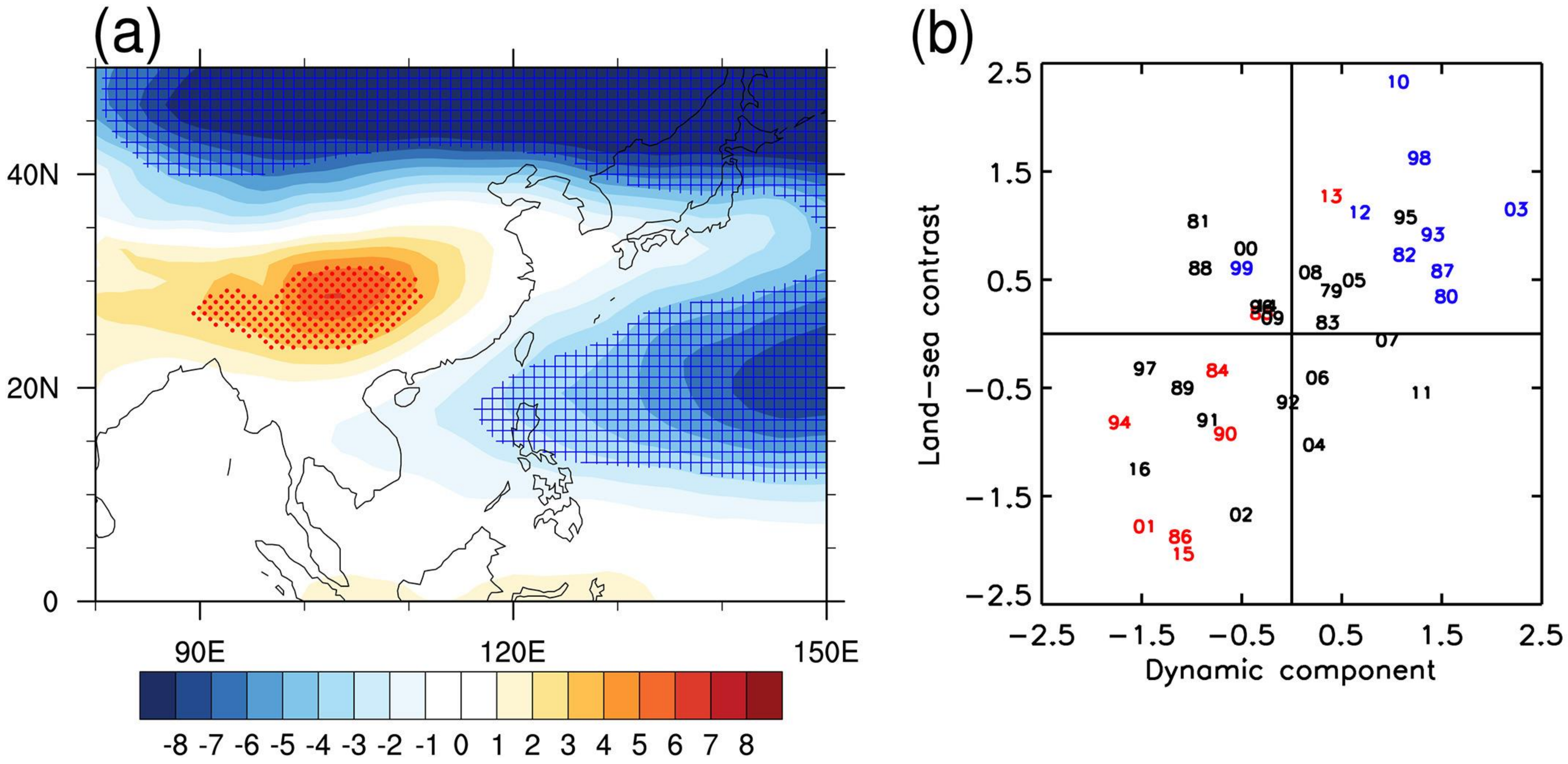

Oh et al., 2018 (JGR)

Dynamic component (dynamic moist convergence + advection)

Dynamic component : $-< \nabla \cdot (\bar{q}_{clim} \delta \bar{V}) >$

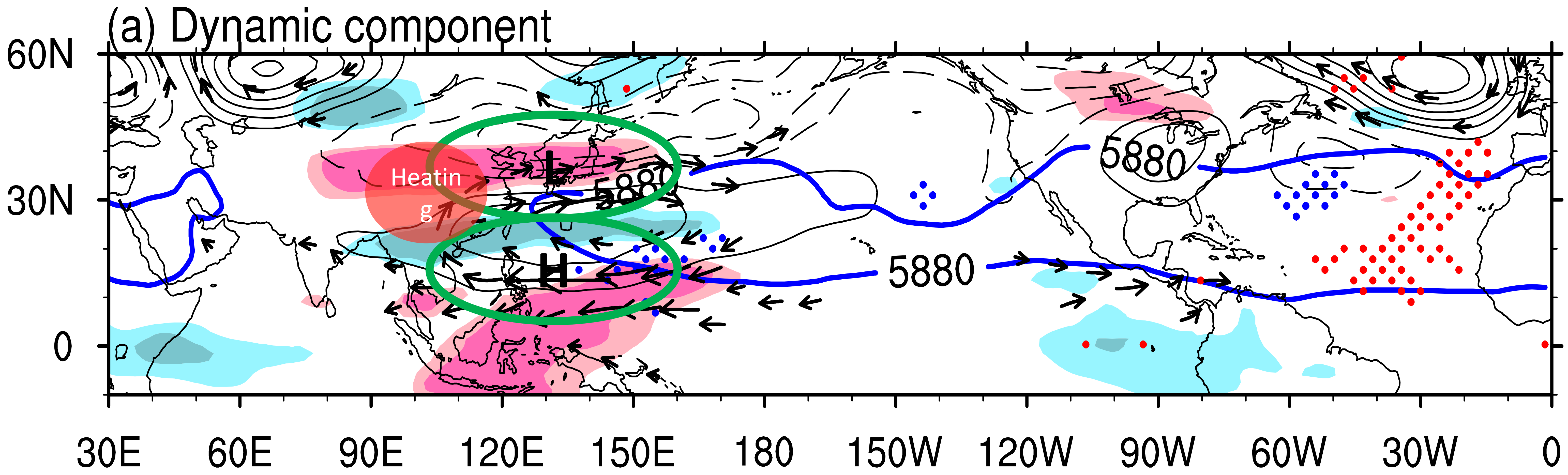

Shading : 200U
Vector : 850UV
Contour : 500Z
Dot : precipitation

- The strong western North Pacific subtropical high (WNPSH) is an essential for determining the variation of the dynamic component over East Asia.
- The accompanied wind at the low-level significantly enhances East Asian frontal system, with a strong cyclonic circulation over East Asia.

Oh et al., 2018 (JGR)

Thermodynamic component

b) Thermodynamic component : $-< \nabla \cdot (\delta \bar{q} \bar{V}_{clim}) >$

mid-latitude Asian summer pattern

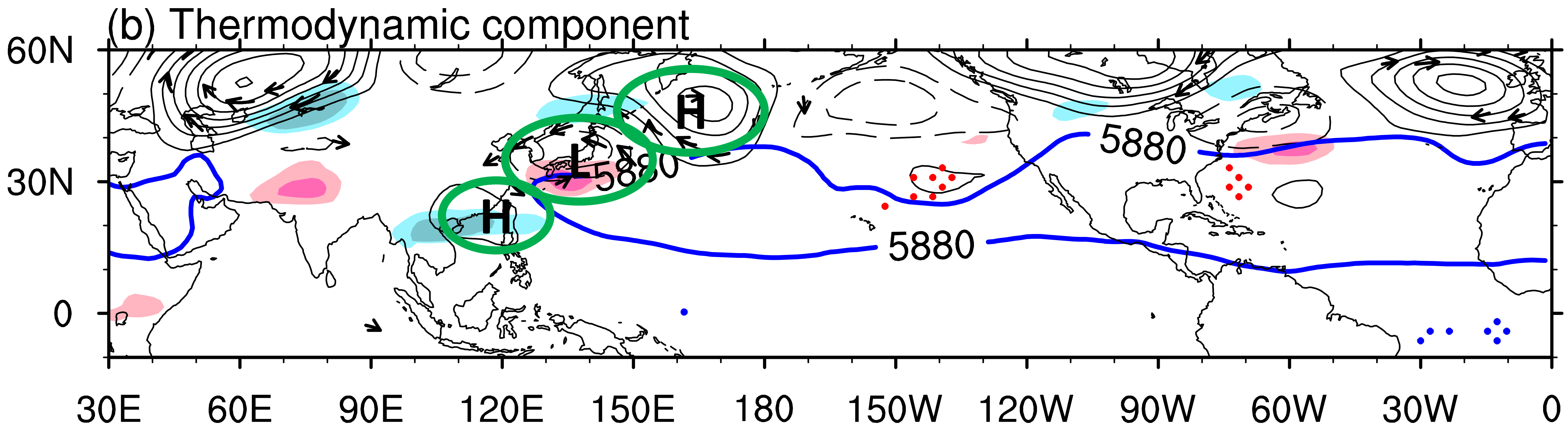

Shading : 200U
Vector : 850UV
Contour : 500Z
Dot : precipitation

- The enhanced wave-train pattern develops an anomalous cyclone over the southern Japan and reinforces Okhotsk high through Rossby wave propagation.
- **The Okhotsk high** induces a positive zonal and meridional gradient of specific humidity toward the EASM region **by blocking eastward propagation of circulation systems.**

Oh et al., 2018 (JGR)

A recipe for extreme precipitation (2018 JGR-Atmos, August Cover story)

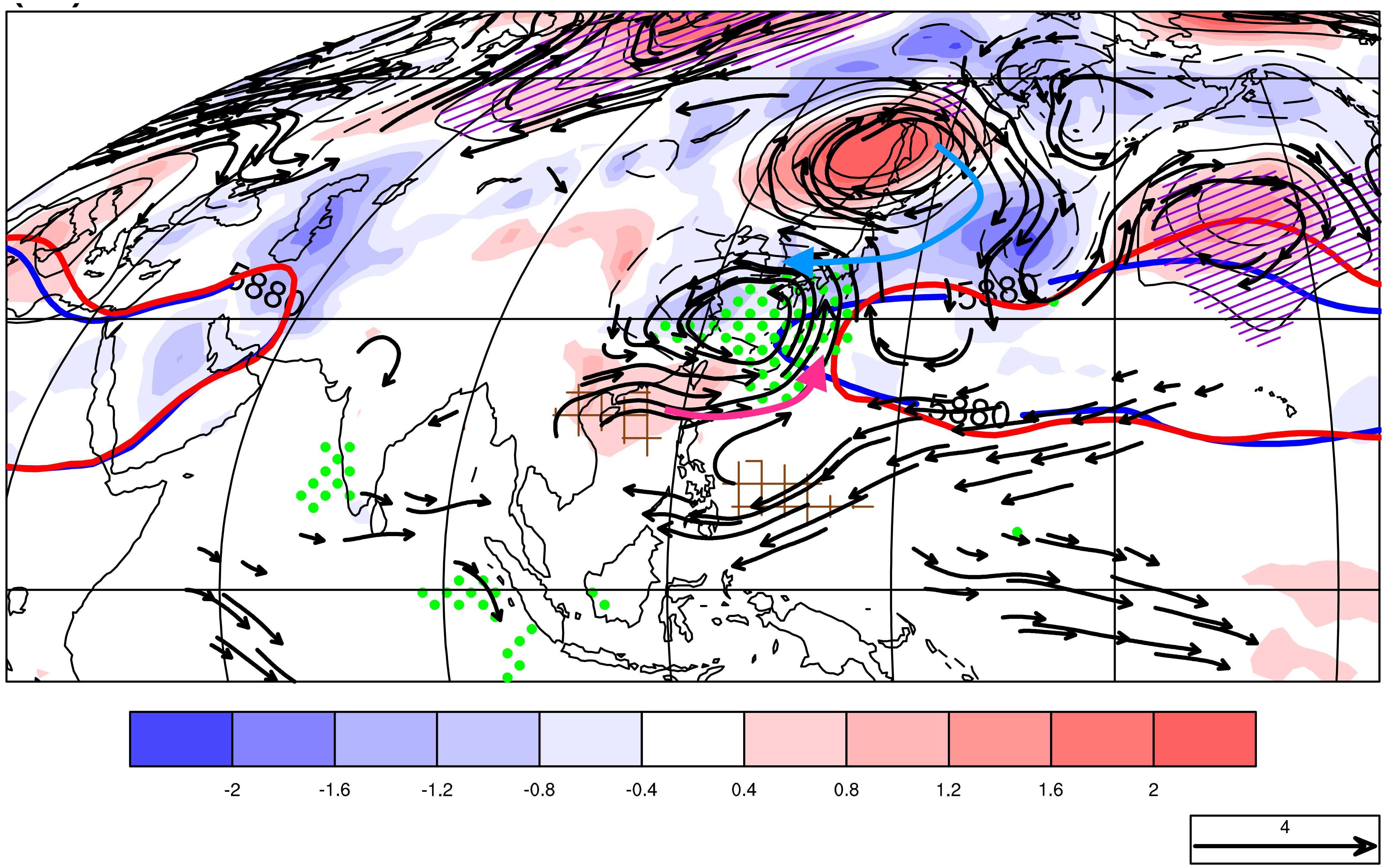

Shading : 850T
Vector : 850UV
Contour : 500Z

- As the wave train at the upper-level is shown to be significant, **it can contribute to development and maintenance of both the Eurasian and Pacific blocking**, resulting in extreme rainfall over East Asia.
- The blocking's frequency and intensity and Okhotsk high affect the strength and location of **cold air intrusion**, which produces heavy rainfall over East Asia.
- When it is combined with the **southerly wind transporting warm and humid air over SCS** to East Asia, extreme heavy rainfall can occur frequently.

Oh et al., 2018 (JGR)

Future changes in precipitation

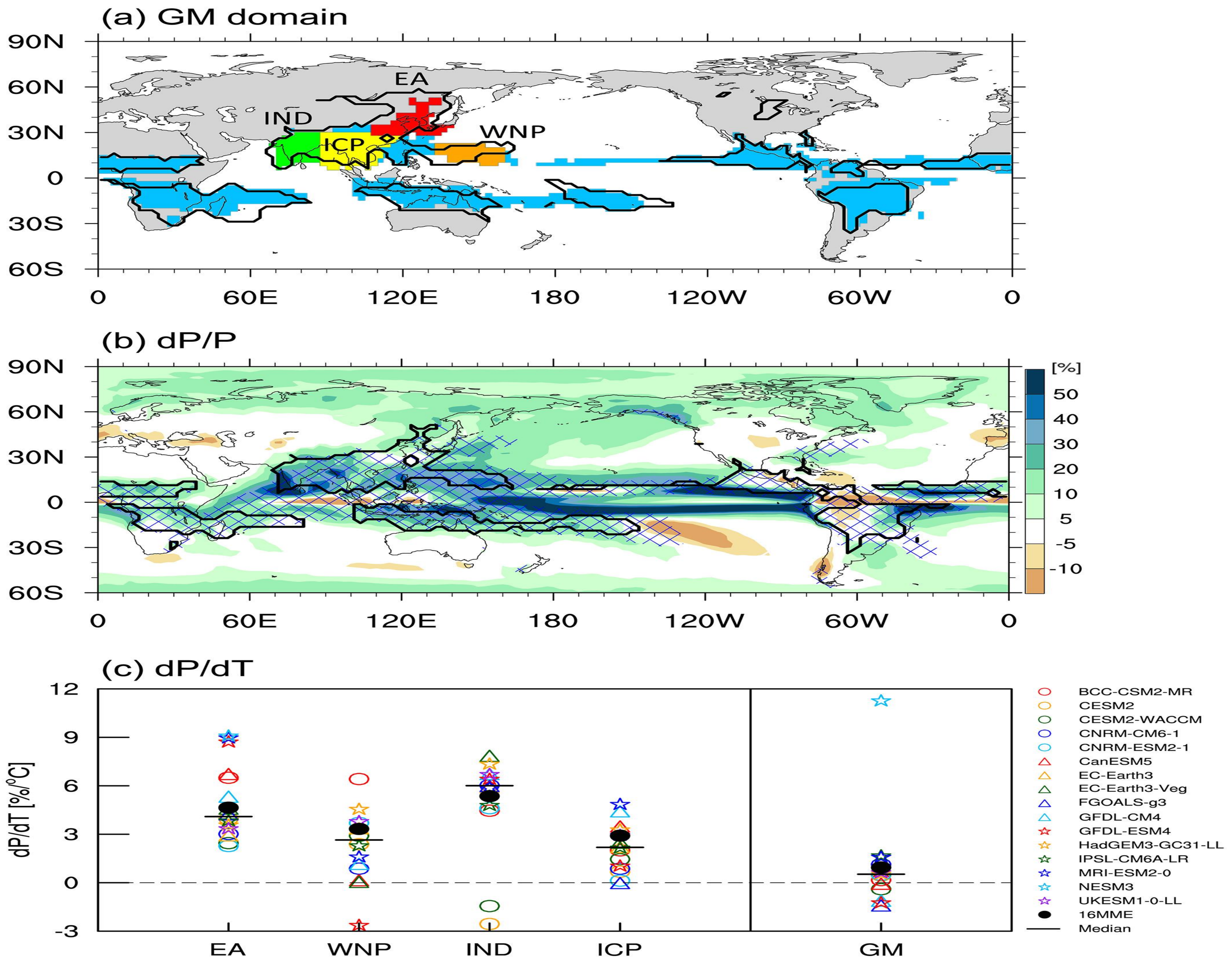

Ha et al., 2020 (GRL)

Projected changes in extreme rainfall

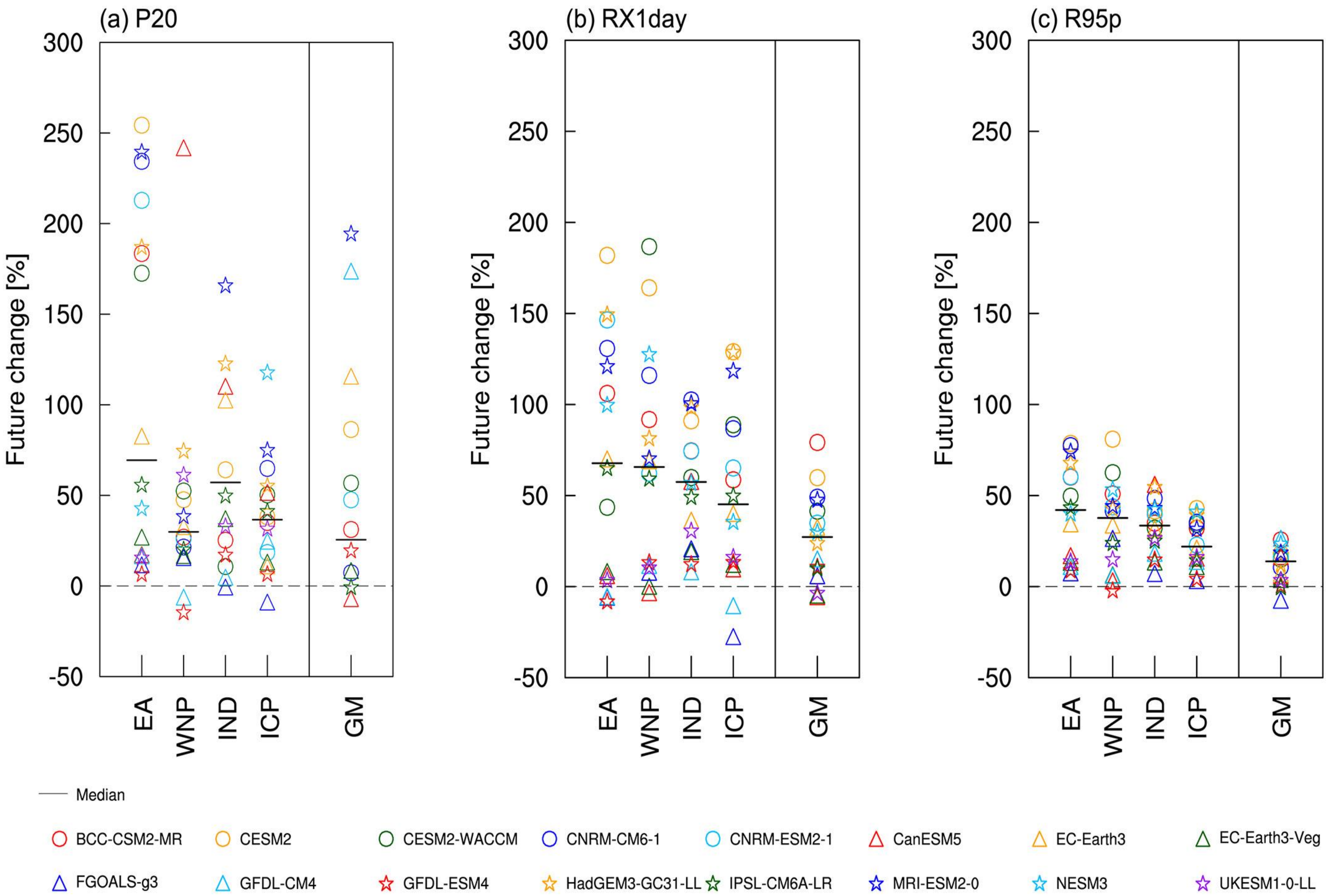

Ha et al., 2020 (GRL)

Feedback attribution analysis

Coupled atmosphere–surface climate feedback–response analysis method (CFRAM, Lu and Cai (2009)**)**

The total energy balance at M atmospheric layers

$$\vec{R} = \vec{S} + \vec{Q}^{nonradiative}$$

The difference between two climate states

$$\Delta \frac{\partial \vec{E}}{\partial t} = \Delta\vec{S} - \Delta\vec{R} + \Delta\vec{Q}^{non-radiative}$$

Change in net rad. heating/cooling

Water vapor, Cloud, Ozone, Albedo

Local temperature differences

$$\Delta\vec{T} = \left(\frac{\partial \vec{R}}{\partial \vec{T}}\right)^{-1} \left\{ \begin{matrix} \Delta\left(\vec{S} - \vec{R}\right)^{(w)} + \Delta\left(\vec{S} - \vec{R}\right)^{(c)} + \Delta\left(\vec{S} - \vec{R}\right)^{(O_3)} + \Delta\vec{S}^{(\alpha)} \\ + \Delta\vec{Q}^{(SH)} + \Delta\vec{Q}^{(LH)} + \Delta\vec{Q}^{(atmos\_dyn)} + \Delta\vec{Q}^{(sfc\_dyn)} \end{matrix} \right\}$$

Planck feedback matrix

Sensible heat, Latent heat, Atmospheric dynamics, Surface dynamics

Change in net non-radiative dyn. heating/cooling

How to calculate the partial temperature changes using CFRAM?

Define surface temperature differences

Differences between **strong dry heatwave years** (HW > 0.5σ & scPDSI < -0.5) and **normal years (excluding strong years)**

Input for radiative transfer model

Annual-mean of input variables

Energy perturbation terms

Using **Fu-Liou radiative transfer model**

$\Delta(\vec{S}-\vec{R})^{(w)}$, $\Delta\vec{S}^{(\alpha)}$, $\Delta(\vec{S}-\vec{R})^{(c)}$, $\Delta(\vec{S}-\vec{R})^{(O_3)}$, $\vec{Q}^{(SH)}$, $\Delta\vec{Q}^{(atmos\_dyn)}$, $\Delta\vec{Q}^{(LH)}$, $\Delta\vec{Q}^{(sfc\_dyn)}$

Decomposition partial temperature changes

Using **CFRAM**

$\Delta\vec{T}^{\text{water vapor}}$, $\Delta\vec{T}^{\text{albedo}}$, $\Delta\vec{T}^{cloud}$, $\Delta\vec{T}^{ozone}$, $\Delta\vec{T}^{\text{SH}}$, $\Delta\vec{T}^{\text{atmos\_dyn}}$, $\Delta\vec{T}^{LH}$, $\Delta\vec{T}^{\text{sfc\_dyn}}$

Ex) To obtain the radiative energy perturbation due to a single process, for example, $\Delta\vec{S}^{(cloud)}$, we run the radiative transfer model **twice**

1) we use the composite **normal state (excluding strong years)**

2) we used the **same composite normal state, but replace the variable associated cloud profile with the corresponding strong dry year state**

3) **Subtracting** the convergence of shortwave radiative flux of the first run from the second run

ICCP

Seo et al., 2021 (ERL)

Feedback attribution to **dry heatwaves**

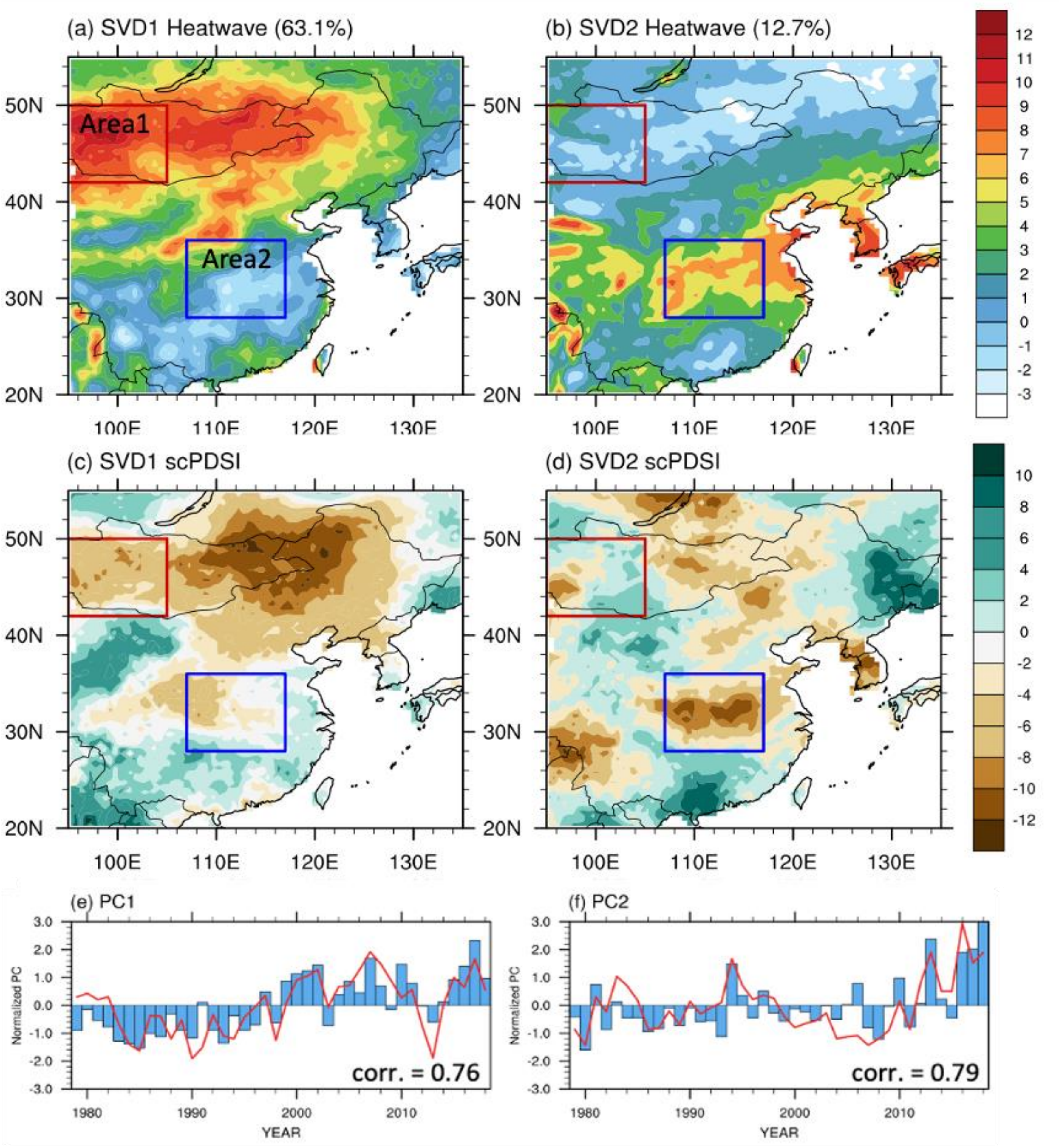

- **Latent heat flux** and **surface dynamic** processes served as positive feedback for surface warming **by reducing the heat release** from the surface to the atmosphere because of **deficient soil moisture** based on dry conditions.
- **Cloud feedback** also led to warm temperature anomalies through **increasing solar insolation** caused by **decreasing cloud amounts** associated with **anomalous high-pressure systems**.

Partial temperature anomalies related to feedback processes

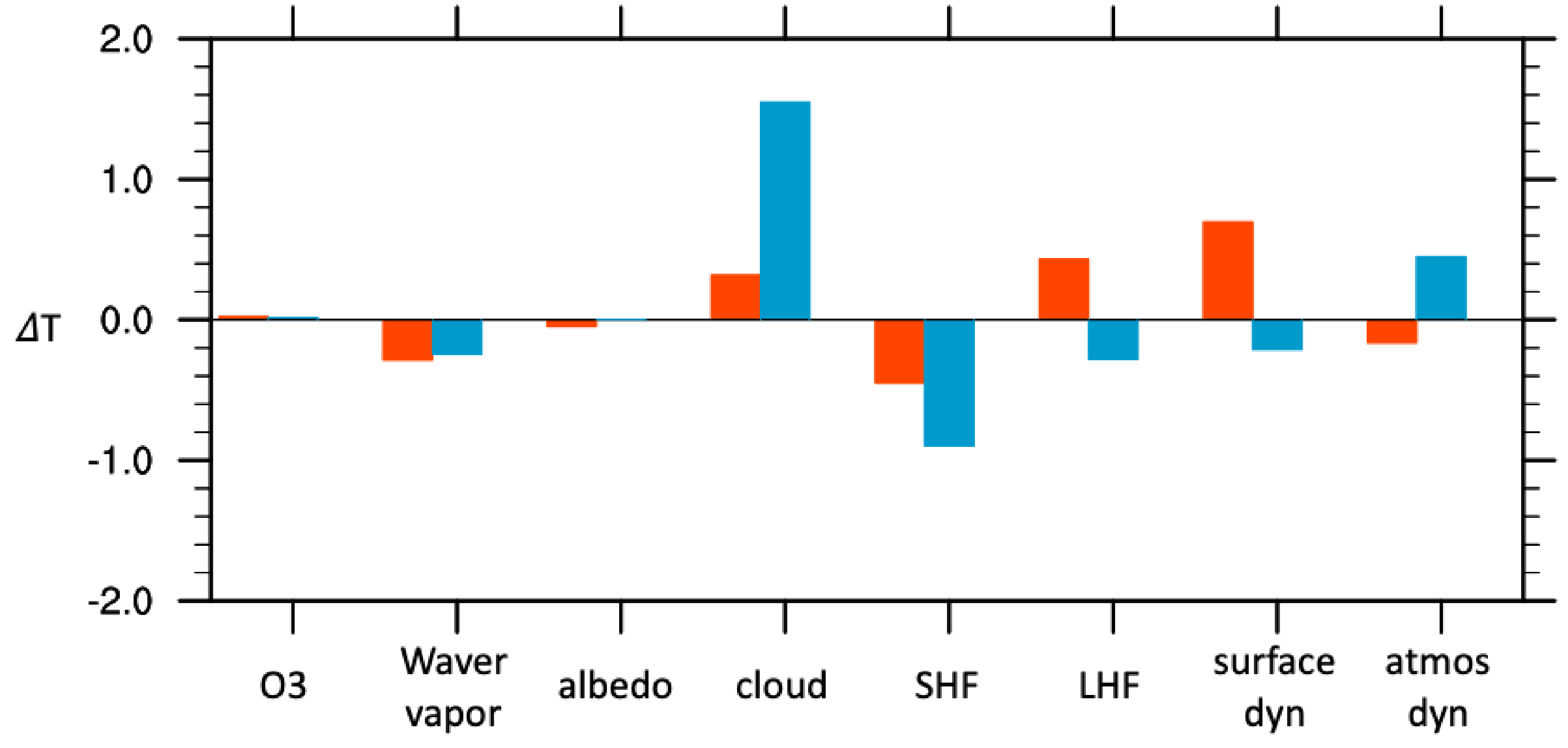

Area1 [95°E-105°E, 42°N-50°N]
Area2 [107°E-117°E, 28°N-36°N]

Seo et al., 2021 (ERL)

Role of Modon-like blocking 2018 from July to August

Large-scale meteorological patterns leading to the prolonged heatwave

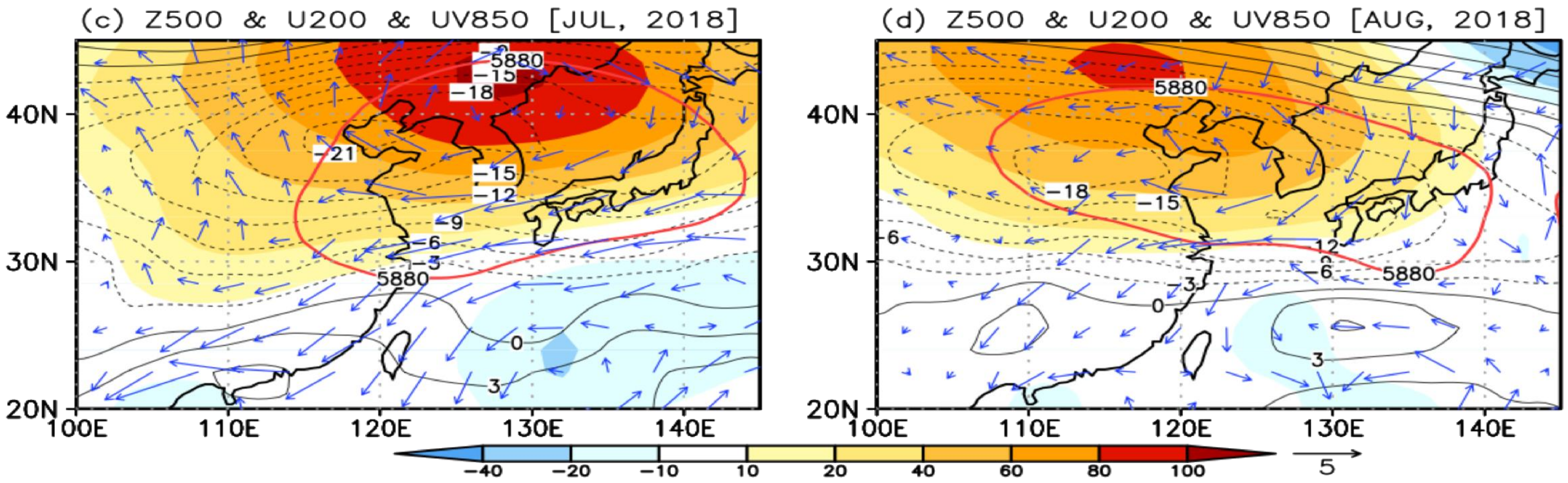

- The HWs in the South Korea are affected by the anticyclonic circulation related to the northern Pacific High (NPH) with negative rainfall anomalies and high Tmax from July to August.
- The results suggest that a **Modon-like blocking** with the northwestward expansion of NPH and a cyclonic anomaly in the east China Sea from July to August causes the strong easterly anomalies and static atmosphere in the mid-latitudes.
- **The expansion of NPH with moisture in the atmosphere** is a key factor in inducing the **persistent heatwave**

Ha et al., 2020 (JMSJ)

Largest loss of moisture from the surface in 2018

Dry condition at the surface with excessive ET

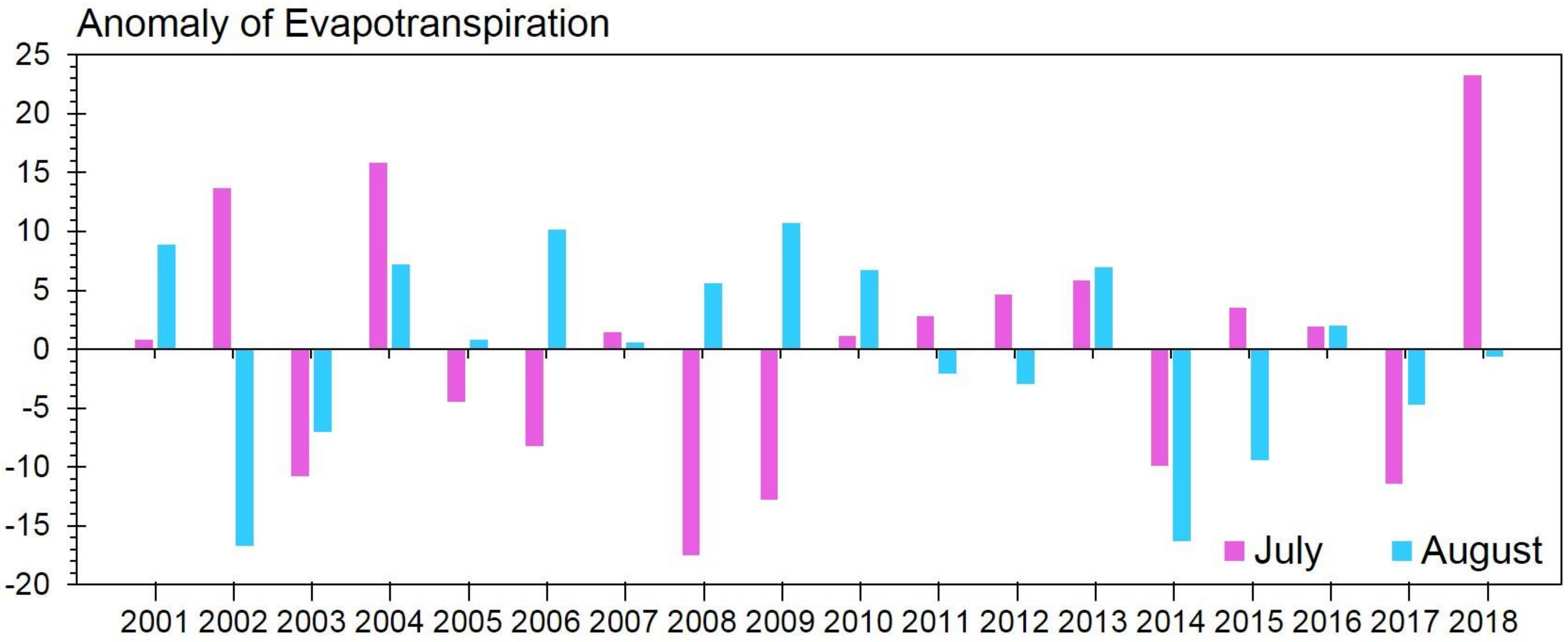

- Despite supply of warm and moist air from south, the mean (anomalous) rainfall and rainy days were 343.4 mm (−12.7 mm) and 7.7 days (−9.4 days), respectively.
- The positive evapotranspiration (ET) anomaly in July 2018 was the largest at 23.5 mm due to high isolation under the low cloud condition and the sinking motion with the expansion of NPH.
- **Prolonged HWs of 2018** were more intense with **compounding effects from the reduction of precipitation and drought with over-ET**

Ha et al., 2020 (JMSJ)

Changes in summer precipitation based on the warm climate

Future changes in precipitation and global temperature over the global monsoon domain

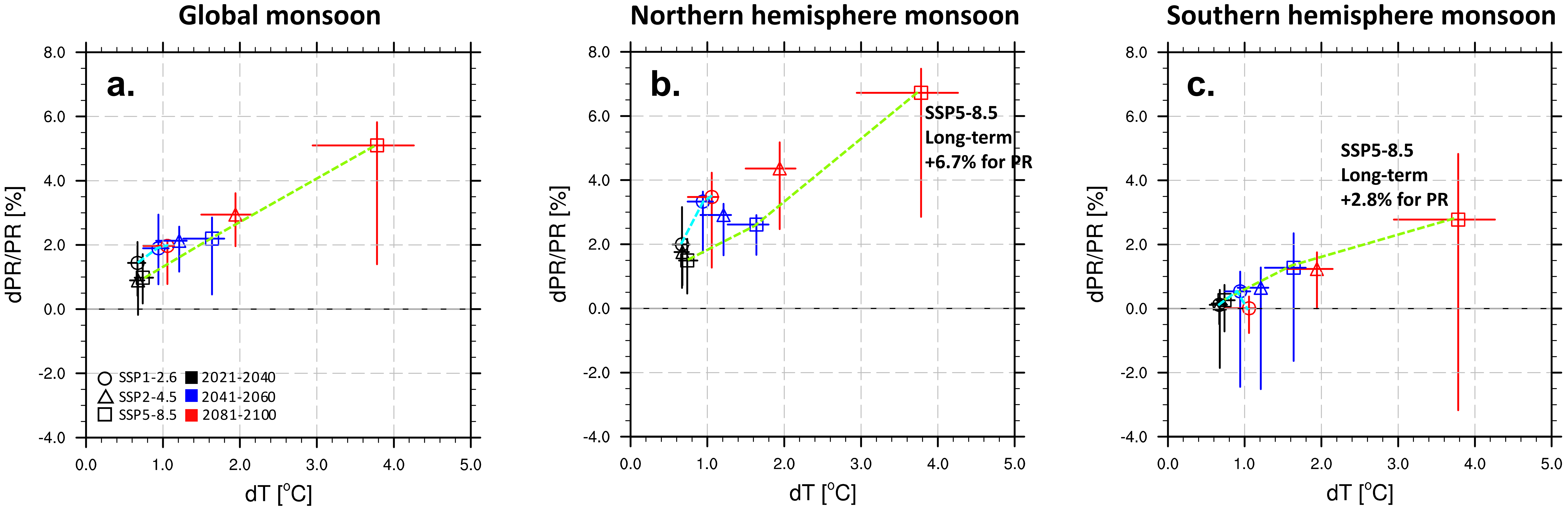

- In terms of emission scenarios and future terms, the changing rate of precipitation is distinct.
- Overall, the rate of precipitation increase under the increasing temperature with nonlinear relation, but less than C-C scale.
- There is largely increased precipitation in the long-term for SSP5-8.5, whereas near-term for SSP1-2.6.
- When we consider the dPR/dT over NHM, the SSP1-2.6 is steeper (4 %/℃) than SSP2-4.5 (2.1 %/℃) and SSP5-8.5 (1.8 %/℃), whereas its percentage change in projected precipitation is lowest among the scenarios.

Moon and Ha, 2020 (npj Clim Atmos Sci)

Changes in summer precipitation based on the warm climate : regional monsoon aspects

Percentage changes in precipitation per one-degree Celsius ($\frac{dP}{dT}$) of global warming in CMIP6 future scenarios

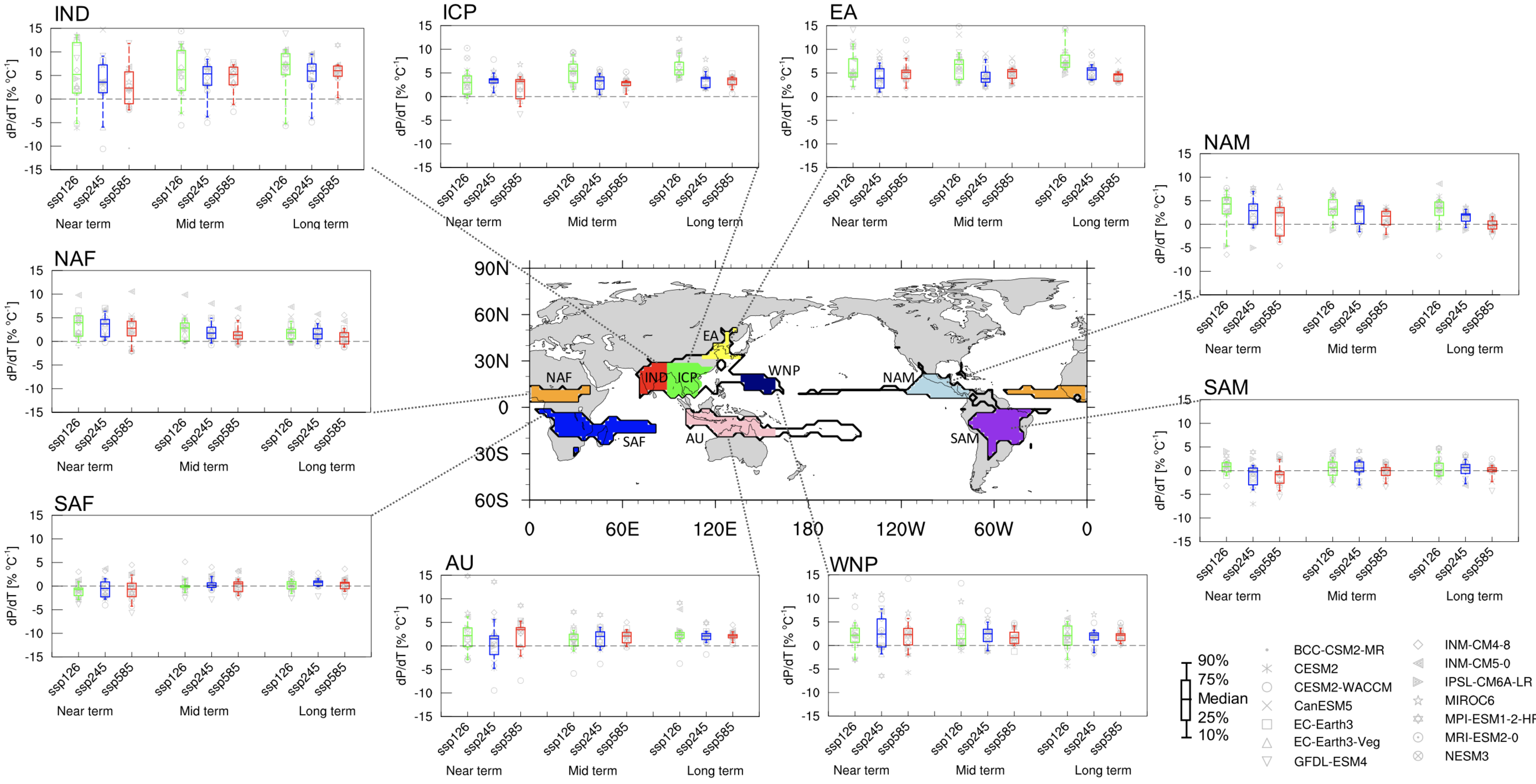

Moon and Ha, 2020 (npj Clim Atmos Sci)

Changes in summer precipitation based on the warm climate : regional monsoon aspects

Percentage changes in precipitation per one-degree Celsius ($\frac{dP}{dT}$) of global warming in CMIP6 future scenarios

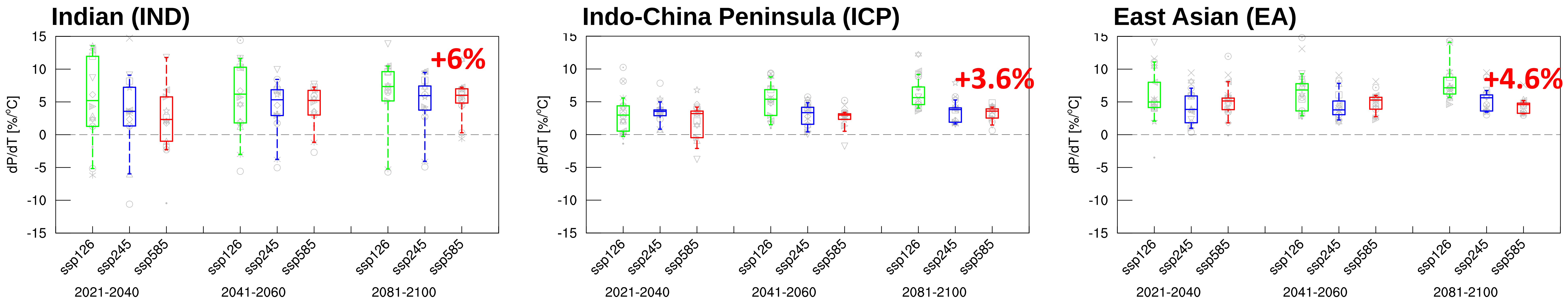

- The percentage change in precipitation is higher:
  over **Indian (+6 %), Indo-China Peninsula (+3.6 %), and East Asian (+4.6%) per 1 ℃ warming in long-term SSP5-8.5 simulation.**
- **An increase of East Asian precipitation in terms of all the scenarios and periods has a high confidence.**
- The maximum increase is in SSP1-2.6 due to the slight increasing temperature (+0.7℃),
  but the spread of models is narrow in SSP5-8.5 in the long-term.

Moon and Ha, 2020 (npj Clim Atmos Sci)

Changes in summer precipitation based on the warm climate : regional monsoon aspects

Percentage changes in precipitation per one-degree Celsius ($\frac{dP}{dT}$) of global warming in CMIP6 future scenarios

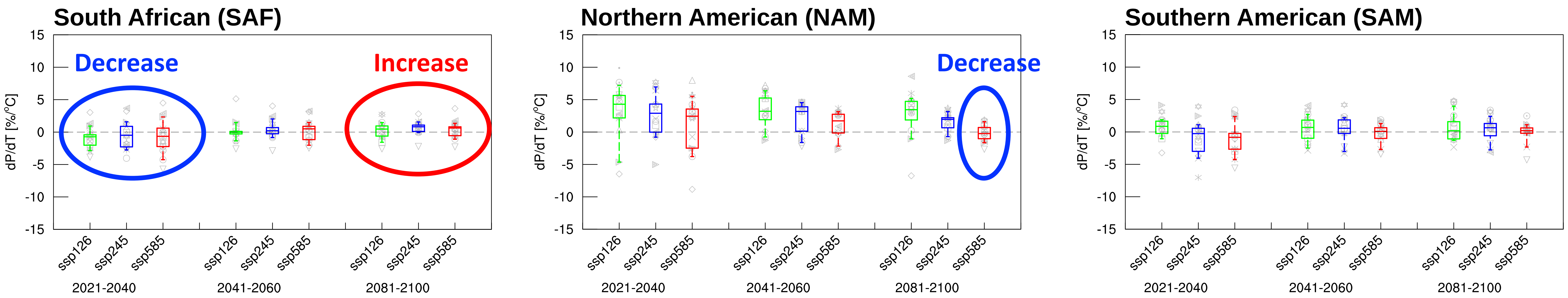

- **Over South African monsoon**, precipitation will **decrease in the near-term** **and slightly increase (+0.6 %℃$^{-1}$) in the long-term.**
- The long-term precipitation over the **Northern American monsoon shows a decreasing rate (-0.2 %℃$^{-1}$) in SSP5-8.5.**
- **The lowest percentage change ($< \pm 1$ %℃$^{-1}$) is shown over the Southern American monsoon.**

- **In sum, most of the regional monsoon precipitations will increase, particularly over Asian monsoon domain.**

Projection of rainy season to climate change

The relationship between **the changes in the rainy season** and **the changes in the precipitation due to temperature rise**

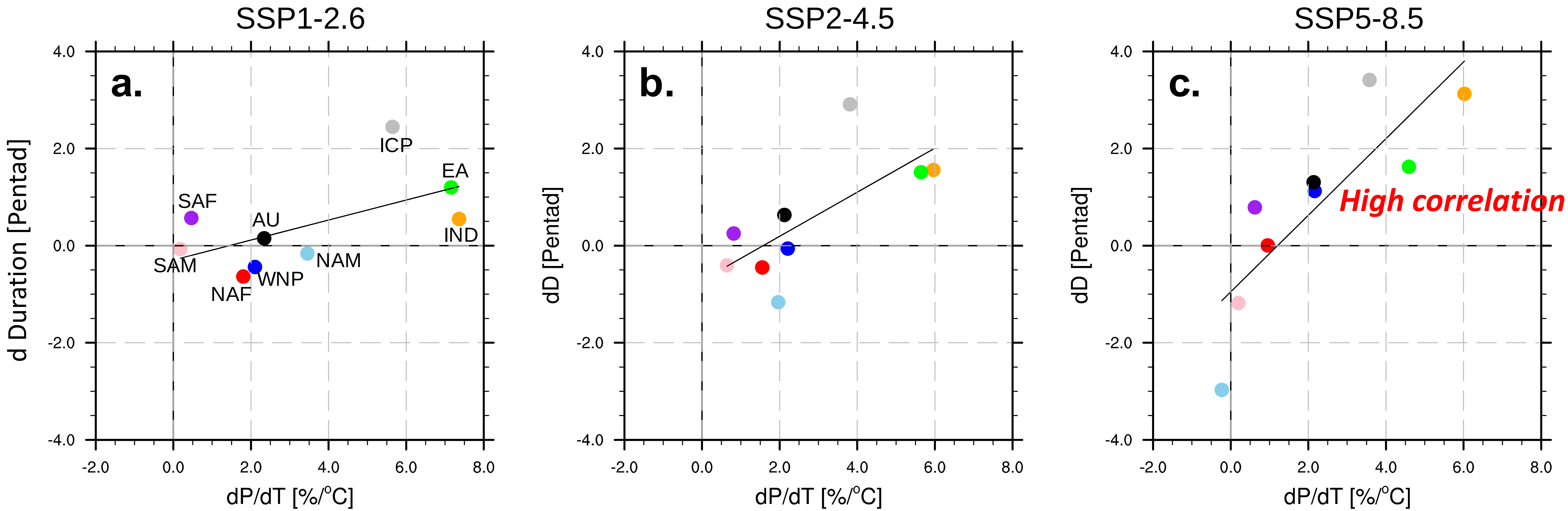

- **The rainy season has a highly positive correlation with the increase of the amount of precipitation** according to one-degree temperature rise.
- The region where has more precipitation increases in the future, will be lengthened the monsoon rainy season.
- **Increasing precipitation – lengthened monsoon duration relationships alarm that the region, where precipitation increases large, shows that prolonged monsoon season, affecting people's lives in another way.**

Moon and Ha, 2020 (npj Clim Atmos Sci)

Contribution of thermodynamic and dynamic effects on changes in PR

Regionally averaged **future changes of each term of the moisture budget equation**

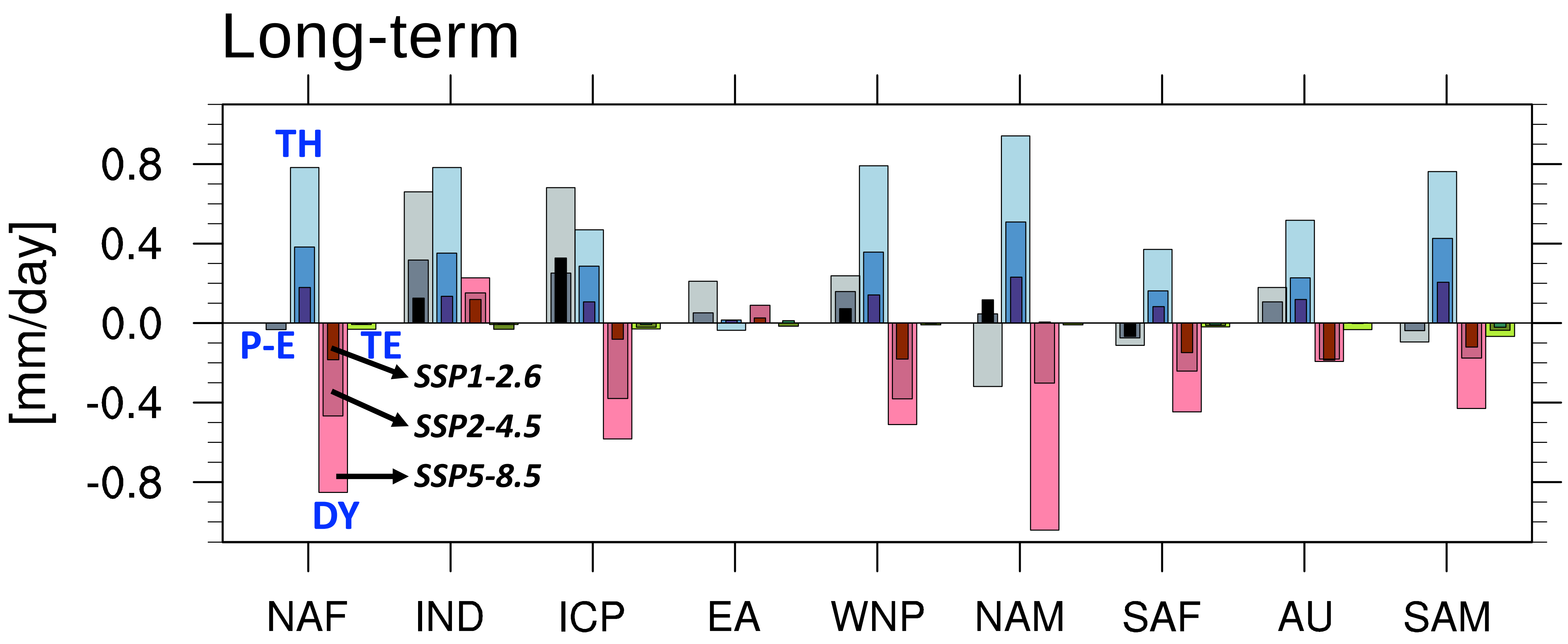

- P-E increase higher over the Asian monsoon domain, particularly in ICP and IND.
- **The positive P-E over most of the monsoon domains is primarily due to the positive thermodynamic (TH) effect associated with warming climate.**
- **The most unique points over EA is the dynamic (DY) term affects positively** and TH influences negatively to increasing summer rainfall.
- **P-E over southern African (SAF) and southern American (SAM) performs a decrease** in future climate **due to the large increase of evapora tion than precipitation**

Moon and Ha, 2020 (npj Clim Atmos Sci)

Summary

- Internal atmospheric fluctuations play a crucial role in generating year-to-year changes in Changma. Dynamic and thermodynamic factors can be used as predictors.

- The distinct large-scale circulation patterns together create favorable conditions for heavy rainfall over East Asia

- Related to TOE, Asian-Australian monsoon (AAM) is still affected by internal variability. Analysis of 16 CMIP6 models indicates that, under the SSP2–4.5 scenario, EASM precipitation will increase at 4.7% °C−1 (Ha et al. 2020b), with dynamic effects more important than thermodynamic effects (Oh et al. 2018; Li et al. 2019). EASM duration is projected to lengthen by about 5 pentads due to earlier onset and delayed retreat (Ha et al. 2020b), which is comparable to previous assessment results (Endo et al. 2012; Kitoh et al. 2013; Moon and Ha 2017).

- Latent heat flux and surface dynamic processes served as positive feedback for surface warming by reducing the heat r elease from the surface to the atmosphere because of deficient soil moisture based on dry conditions. Cloud feedback also led to warm temperature anomalies through increasing solar insolation caused by decreasing cloud amounts asso ciated with anomalous high-pressure systems.

- Generally, heat stress index shows increasing over the Korean peninsula with increasing CO_2.